

OBSERVATIONS OF THE STRATOSPHERIC AEROSOL LAYER DUE TO MT. PINATUBO ERUPTION AT A NETWORK OF LIDAR STATIONS

V.V. Zuev, V.E. Zuev, and V.N. Marichev

*Institute of Atmospheric Optics,
Siberian Branch of the Russian Academy of Sciences, Tomsk
Received June 10, 1993*

An overview of papers devoted to studies of the stratospheric aerosols due to Pinatubo eruption presented at the 16th ILRC (Massachusetts, USA, July 20–24, 1992) is given in this paper. The mass of gases and aerosol substances erupted from the Mt. Pinatubo volcano exceeds the powers of any recently observed eruptive clouds and can cause essential climatic changes on the global scale.

A series of eruptions of the Philippine Mt. Pinatubo volcano in June 1991 climaxed in the eruption on June 15. This eruption, with respect to power of the aerosol and gas volcanic cloud delivered into the stratosphere, was much more huge than those in recent years and yielded about 20 megatonnes of SO₂ which is about three times the amount produced by the eruption of El Chichon in 1982 (Bluth et al., Ref. 1). Such a great amount of aerosol in the stratosphere could have many impacts on the Earth's radiation budget as a whole and cause many climatic effects. This event has become a subject of scientific interest to studies of the development and propagation of this stratospheric cloud on a global scale. Currently available lidar stations in the world as well as mobile lidars operating in an routine measurement mode made it possible to study at length spatiotemporal distribution of the stratospheric volcanic layer. The geography of observations covers Europe (Germany and Italy), North America (the USA and Canada), and Asia (Japan, Russia, and China) in the Northern hemisphere and southeastern Australia in the Southern hemisphere.

The results of lidar measurements are represented by vertical profiles of aerosol coefficients of the total and backward scattering, scattering ratio, and an optical depth of the volcanic layer. Of fundamental importance was the use of polarization characteristics of light scattering and multiwave length sensing which extended a knowledge of microphysics of aerosol particles including their shapes and size distribution.

Long-term routine observations started prior to the Pinatubo eruption enabled one to follow the formation of a volcanic aerosol layer and its propagation over continents and its later spreading and sink.

The measurement results obtained at the lidar stations and mobile lidars have the following common features.

(1) The emergence of the first short-lived volcanic layer at lower altitudes (from tropopause down to 17–20 km) and the second one with an extended period of life at altitudes of from 21 to 30 km and higher.

(2) A spherical shape of aerosol particles in the basic volcanic layer and irregular-shaped particles below the layer.

(3) Use of a Raman-lidar return signal from molecular nitrogen for separating out the aerosol and molecular components of the total scattering signal.

VOLCANIC STRATOSPHERIC LAYER OVER EUROPE

The aerosol volcanic layer over Europe was monitored from lidar stations at Research centers: GKSS in Northern Germany, Geesthacht (53.5°N, 10.5°E), and ENEA in Italy, Frascati (41.8°N, 12.7°E).

The GKSS lidar station measurements² were carried out since August 1991 based on elastic and Raman scattering of a XeCl excimer laser radiation at 308 and 332 nm (from N₂). Use of a double frequency technique for detecting lidar returns up to 35 km height allowed one to separate aerosol extinction and backscatter and restore the profile of extinction (α) and backscatter (β_{π}) coefficients and of the backscattering ratio R in the perturbed lower stratosphere. Figure 1 shows the dynamics of stratospheric aerosol for the time period from August 1991 till December 1992. Until November the aerosol particle density is moderately enhanced. The scattering ratio was below 2 which corresponded to values 6 and 12 for $\lambda = 550$ and 770 nm, and the top height was between 21 and 25 km. A rapid increase of light scattering by particles was observed in the beginning of December 1991. On December 8, the aerosol layer reached up to 30.5 km and its optical depth was 0.3 with maximum $R = 3$ for $\lambda = 308$ nm. The increase of the aerosol content in the stratosphere could result from circulation when strongly mixed air masses began to move to the north in the fall of 1991 and reached 53°N in December. In the presence of a more dense aerosol cloud the stratosphere got cooler that was confirmed by radiosonde measurements. Very low temperatures down to -83°C were observed between 25 and 33 km heights during December and January.

Measurements of January 17, 1992 showed the stratospheric aerosol layer to extend from 17.5 to 22 km with lidar ratio between 20 and 30 sr, optical depth of 0.15, and $\beta_{\pi} \approx 0.001 \text{ km}^{-1}\text{sr}^{-1}$. Since the measurements were made at 308 nm wavelength the ozone absorption was taken into account based on the results obtained at the nearest ozone-sounding station Mt. Hohenpeisenberg (48°N).

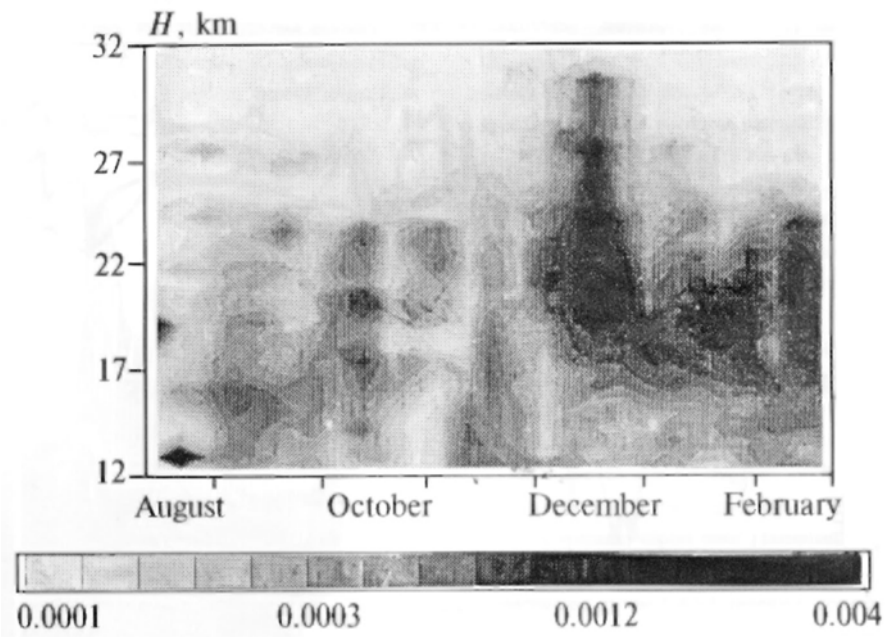


FIG. 1. Evolution of the stratospheric aerosol layer in terms of $\beta_{\pi a}$ at $\lambda = 308$ nm. Time resolution is 1 week, range resolution is 600 m. The number of laser shots is 1.5×10^6 and time of data accumulation is 2 h.

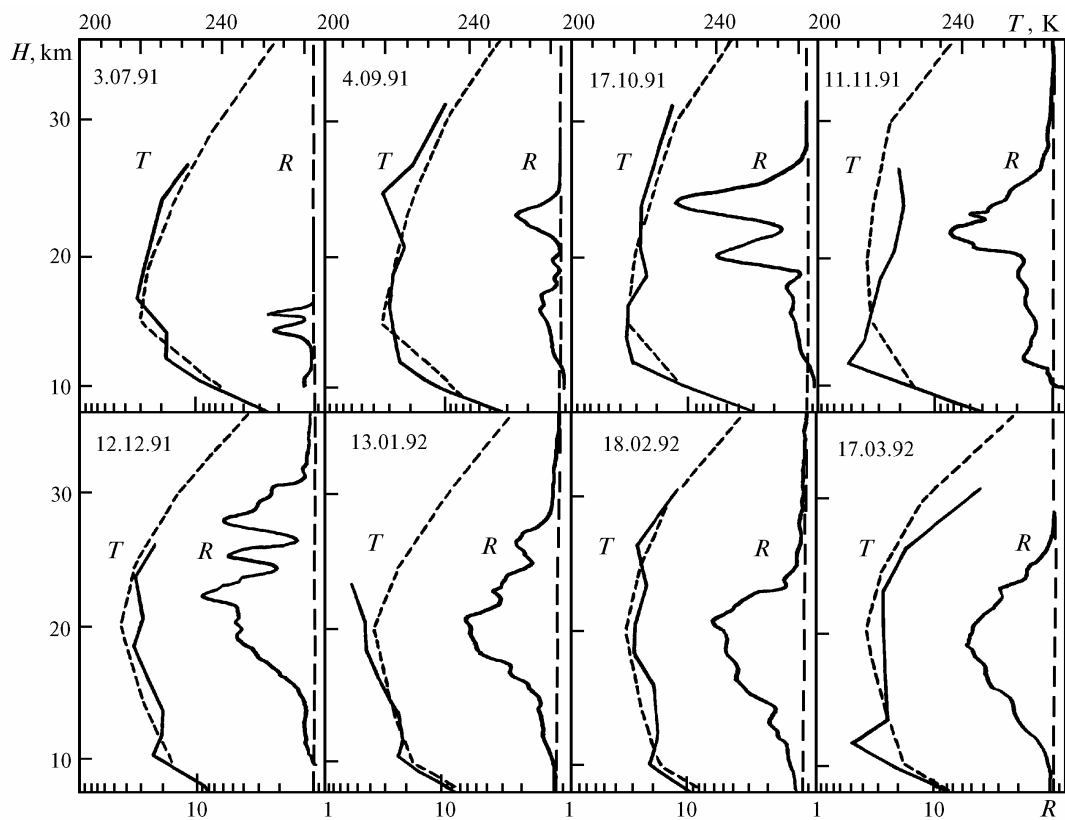


FIG. 2. Temperature profile T and ratio R . Solid line is for radiosonde data and a dotted line is the CIRA model.

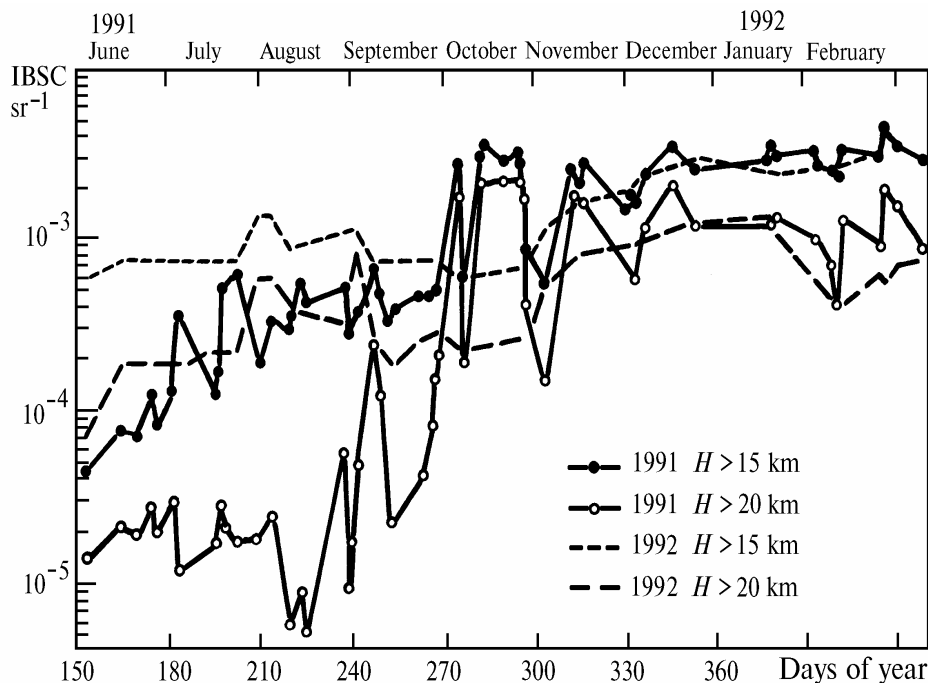


FIG. 3.

At the beginning of measurements in August 1991, very low lidar ratios around 5 sr were observed. Such disagreement with the Mie theory was probably caused by nonspherical particles like ice crystals in the stratosphere. Several months after Mt. Pinatubo eruptions the lidar ratio noticeably increased to 10–30 due to the stratospheric aerosol layer consisting of spherical sulfide particles. Since heavy nonspherical particles had left the stratosphere under these conditions the particle radii can be estimated using the Mie theory. The measurements are in a good agreement with the numerical calculations made for $\lambda = 532$ nm based on the particle size spectrum measured by Jäger and Hofmann.³

Observations of the volcanic cloud over Frascati (Italy, 41.8°N, 12.7°E) were performed⁴ since July 1991. Their lidar system is based on a YAG laser ($\lambda = 532$ nm and pulse energy 200 mJ) and a 50 cm diameter Cassegrainian telescope. Evolution of the local volcanic layer is depicted in Fig. 2. It is seen that 20 days after the Pinatubo eruptions, the aerosol layer was detected at 14 km altitude over Frascati. The upper portion of the cloud at altitude of 23 km was observed on September 4, 1991. The maximum scattering ratio ($R \approx 14$) was measured on October 17. At that time the volcanic cloud extended from the tropopause up to 30 km.

The analysis of the temporal behavior of the integral backscattering coefficient (IBSC) presented in Fig. 3 shows that three and a half months after the eruption the aerosol perturbation generated by Pinatubo reached and exceeded the maximum loads observed 11 months after the El Chichon event. Thus the rate of increase of the Pinatubo aerosol content was three times higher than that in the El Chichon stratospheric layer. It is seen from Fig. 3 that perturbations generated by El Chichon volcano are a lower limit of those which follows the Pinatubo eruption. The highest altitude where the eruptive cloud was observed is 31 km and it was reached by the middle of December.

THE VOLCANIC STRATOSPHERIC LAYER OVER NORTH AMERICA

Observations of the volcanic stratospheric layer over North America and its southeastern maritime zone were made from lidar stations in Toronto (Canada), Hampton, and southeastern Kansas (USA) as well as with a NASA airborne lidar (USA).

In Toronto (42.8°E, 79.5°W) the routine observations have been carried out since March 1991 using the differential absorption (XeCl-laser) and elastic scattering (second harmonic of a Nd:YAG laser) lidars.⁵ In the period from March 1991 till March 1992 more than 90 night measurements of the stratospheric aerosol have been carried out. The Pinatubo aerosol cloud reached Toronto on July 21, 1991 forming two layers at 17 and 22 km altitudes. Figures 4 and 5 show three-dimensional representation of its dynamics using scattering ratio measured at 532 and 353 nm. As seen in the figures, the maximum value of R did not exceed 5 at both these wavelengths. Fine structure of R profile at 532 nm is better developed than that at 353 nm because of stronger molecular scattering at the latter wavelength ($\beta_{\text{pm}} \sim \lambda^4$). The layer at 17 km existed till the end of October 1991. The average backscattering ratios in this layer are $R_{353} = 1.3$ and $R_{532} = 2.2$. The layer at 22 km disappeared on the 240th day of the year. The average backscattering ratio in this layer is about 2.7 (532 nm), i.e., higher than in the lower layer. On the 260th a layer appeared, again a few days, at about 23 km. By the end of September a very strong layer was detected at about 24 km altitude with $R = 5$ (532) and $R = 2$ (353 nm). Then, on the 305th day, this layer was observed again and its density increased more rapidly yielding $R = 5$ at $\lambda = 353$ nm. It is quite probable that this layer had travelled around the Earth in 35 days. The growth of R could happen because of the particles growth during the travel. Estimates show that the velocity of such

a travel should be 830 km/day (10° a day) or about 10 m/s. For a comparison, McCormick found that the main eruption plume was moving east at a speed of 30 and 20 m/s in the second week of July and first week of August 1991. However, it should be taken into account that in this case the wind regime was different than that in the above mentioned case.

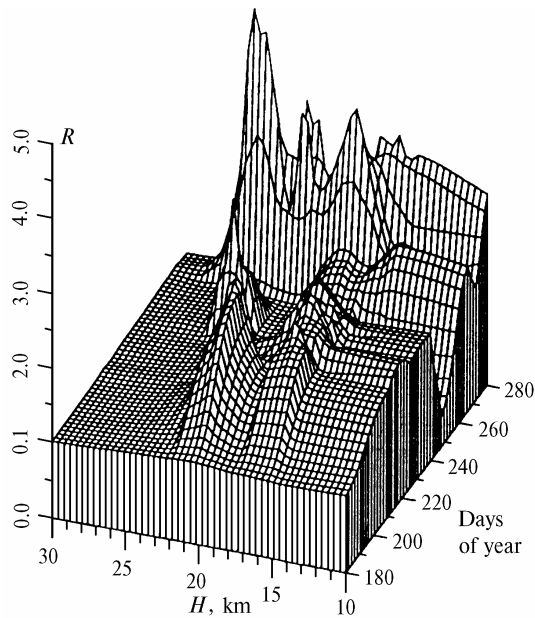


FIG. 4. Variations in R at $\lambda = 532$ nm between June 29, 1991 (180th day) and October 7, 1991 (280th day after eruption).

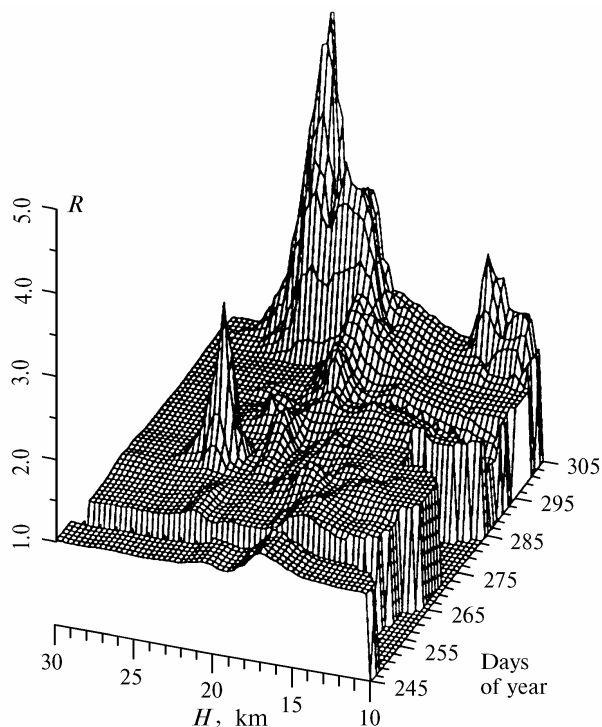


FIG. 5. Variation in R at $\lambda = 353$ nm between September 2, 1991 (245th day) and October 31, 1991 (304th day).

To detect deviations of particle shapes from sphere two channels were used for recording of parallel and perpendicular polarized components of scattering. Since backscattering by spherical particles does not change the polarization the ratio of a cross-polarized component to the parallel one $\delta = P_{\perp}/P_{\parallel}$ is indicative of particles nonsphericity. Figure 6 shows the profiles R and δ as an example of such measurements. Profiles of these values have quite opposite behaviors. Thus the maximum ($R = 4$) at 24 km corresponds to minimum of the depolarization ($\delta = 0.6\%$) while the largest peak ($R = 1.2$) at 19 km corresponds to maximum of the depolarization ($\delta = 5\%$) profile at this height. If we take into account that in clear air $\delta = 1.4\%$, then it becomes obvious that in the main volcanic layer there are only spherical particles, probably $\text{H}_2\text{SO}_4/\text{H}_2\text{O}$ droplets. In a weaker layer at 19 km there is a great amount of nonspherical particles which may be of a solid crystal material.

A volcanic cloud over Hampton (Virginia, 37.1°N , 76.3°W) was examined using a ruby lidar with a 48-inch telescope constructed at the NASA research center.⁶ To separate aerosol and molecular components of scattering they used, as it was made in Ref. 6, the pressure and temperature profiles derived from radiosonde measurements. The routine observations were started on July 13. Vertical distribution, intensity, and propagation of the Pinatubo volcanic cloud were analyzed based on the parameter of the scattering ratio R . The volcanic aerosol layer was first detected on August 3, 1991 and the background content of stratospheric aerosol was measured on July 18. Clouds in the troposphere prevented observations between July 18 and August 3. Between August 3 and March 11, 1992, 40 sets of nighttime measurements were taken. Figure 7 shows 20 profiles which describe variations in aerosol content in the stratosphere between August 3, 1991 and February 28, 1992. A weak layer appeared on August 3 at an altitude lower than 20 km and the first sighting of the second layer above 24 km occurred on August 24. Even though the power and vertical distribution of the aerosol layer varied widely day to day, a general increase in the amount of aerosol was revealed during this period (August 1991 – February 1992). Pinatubo aerosol layers at altitudes above 30 km were first detected on October 31. In December, 1991 lidar returns were calibrated not by signals from the tropopause but by signals from altitudes above 30 km since a significant increase of aerosol in the troposphere occurred by this time. An extremely dense layer ($R = 34$) was observed at 22.4 km altitude on February 20. It is likely that this layer was a tropical layer from the Pinatubo eruption cloud transported during the winter from low to middle latitudes. The scattering ratio profiles obtained during half an year since the Pinatubo eruption are indicative of a gradual descent and broadening of the Pinatubo aerosol layer.

The peculiarities of formation and behavior of volcanic clouds from El Chichon and Pinatubo during 300 days after their eruptions were compared based on the analysis of time history of integrated backscattering coefficient (IBSC) (Fig. 8). In both cases continuous increase of IBSC is observed due to formation of aerosol particles from gas and poleward transport of the aerosol from the tropics. The background aerosol level preceding the eruption of Pinatubo was lower than the level preceding the El Chichon event. The first volcanic aerosol layer from El Chichon and that from Pinatubo reached Hampton in 42 and 48 days, respectively, that means that the velocities of their transportation in the stratosphere are close to each other. The maximum of IBSC in the layer from Pinatubo occurred 250 days after the eruption shows that Pinatubo yielded the aerosol over burdening which was twice as large as that from El Chichon reached on 245th day after its eruption.

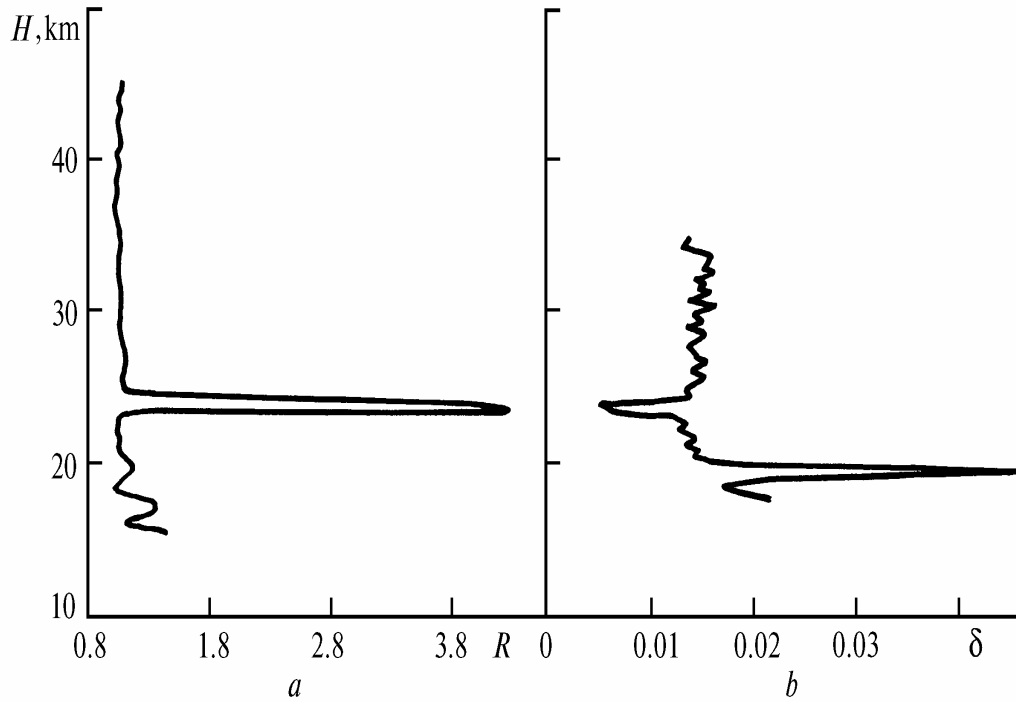


FIG. 6. Values of R (a) and δ (b) at $\lambda = 532$ nm measured above Toronto on September 4, 1991.

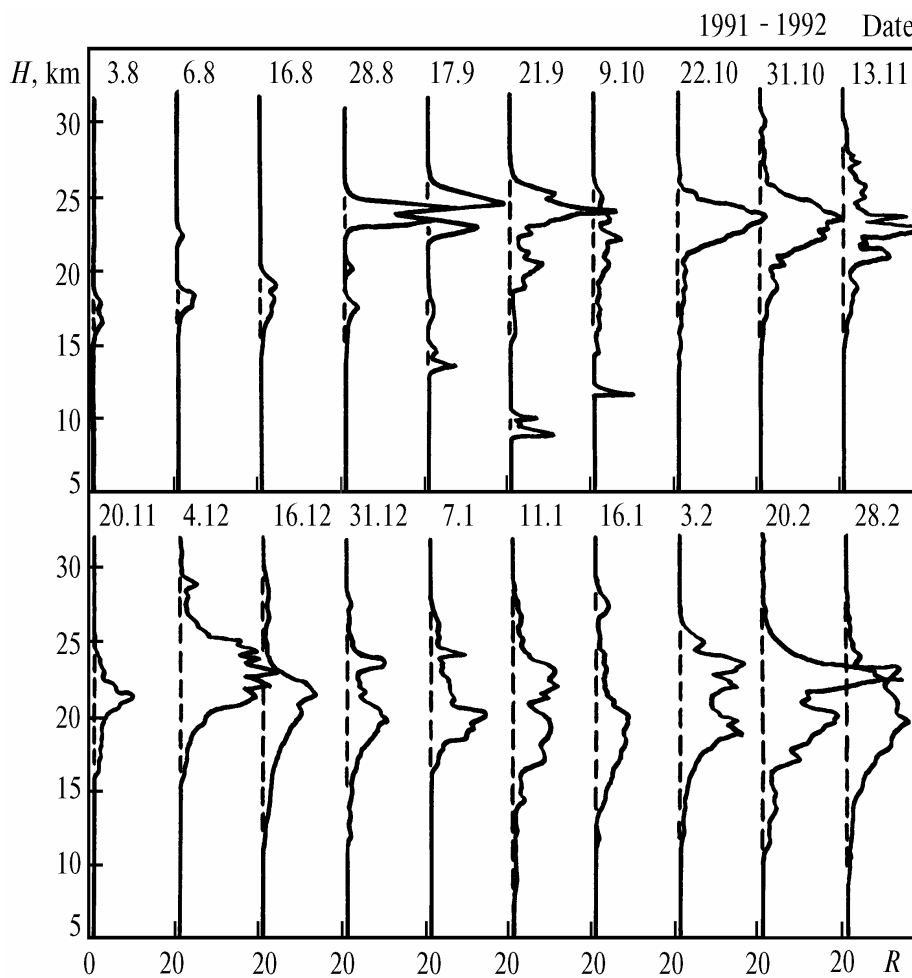


FIG. 7. Profiles of R taken by the LaRC lidar system between August 3, 1991 and February 28, 1992.

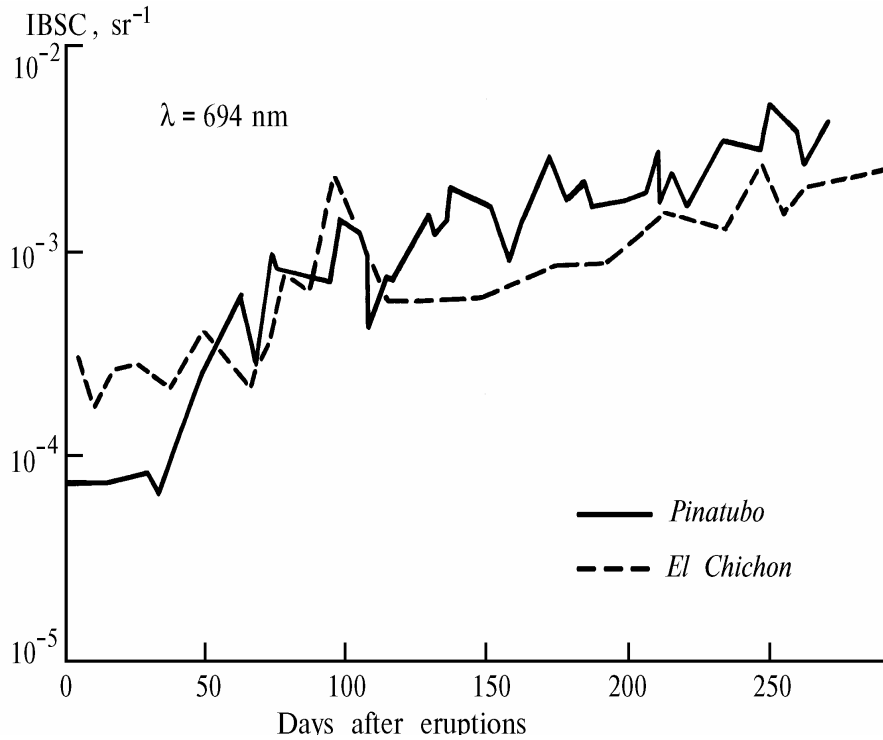


FIG. 8. Time history of IBSC in the stratosphere measured with LaRC lidar following the eruptions of El Chichon and Pinatubo.

Depicted in Fig. 9, for a comparison, are vertical profiles of aerosol scattering coefficient derived from the lidar and the SAGE-II satellite data. The scattering coefficients obtained from lidar data were then recalculated for $\lambda = 1.02 \mu\text{m}$. An excellent agreement between the profiles of scattering coefficient, measured with the lidar and calculated from SAGE-II data was observed for data on October 24, 1991. The same is with the data obtained on December 31. It should be noted, however, that the signals from the satellite were obtained from 25 km and higher while the lidar returns were detected within the altitude range from 5 to 35 km. The experiment illustrates good potentials of the lidar and SAGE-II satellite in determining altitudes and stratospheric aerosol content because the lidar data supplement a lower part of the aerosol scattering profile and are checked against the satellite data in the upper part of the profile.

The program on examining the stratospheric volcanic layer accomplished at NASA Langley Research Center in Hampton was extended at the expense of multifrequency sensing of the atmosphere.⁷ The lidar system employed a three-wavelength (1064, 532, and 355 nm) Nd:YAG laser and a 14.5-inch receiving telescope, an ADC, a mechanic chopper, and a video camera for scanning the sky.

The layer observations were begun at the end of February 1992. Lidar return calibration by molecular scattering was performed using a signal from the upper tropospheric region and taking into account the aerosol model of the atmosphere. Because of low signal-to-noise ratios at altitudes above 25 km it was impossible to normalize the profile using signal from these altitudes. An example of three-wavelength sensing in the form of scattering ratio profiles (February 27, 1992) is shown in Fig. 10.

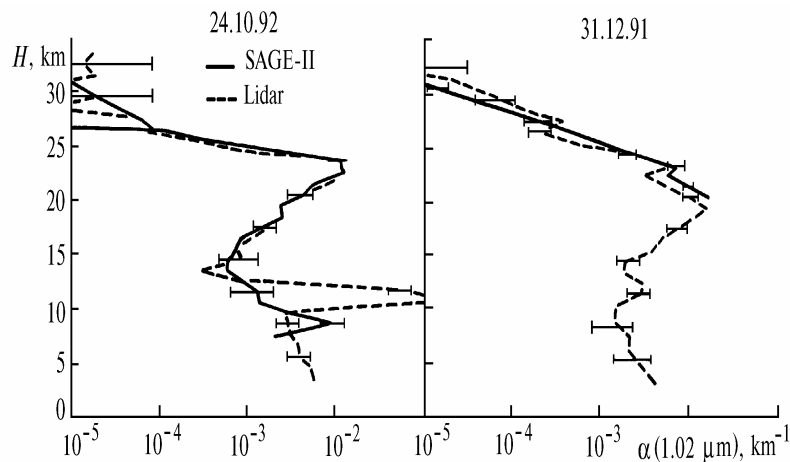


FIG. 9. Comparison of the profiles of aerosol extinction acquired with SAGE-II and lidar at 1.02 μm.

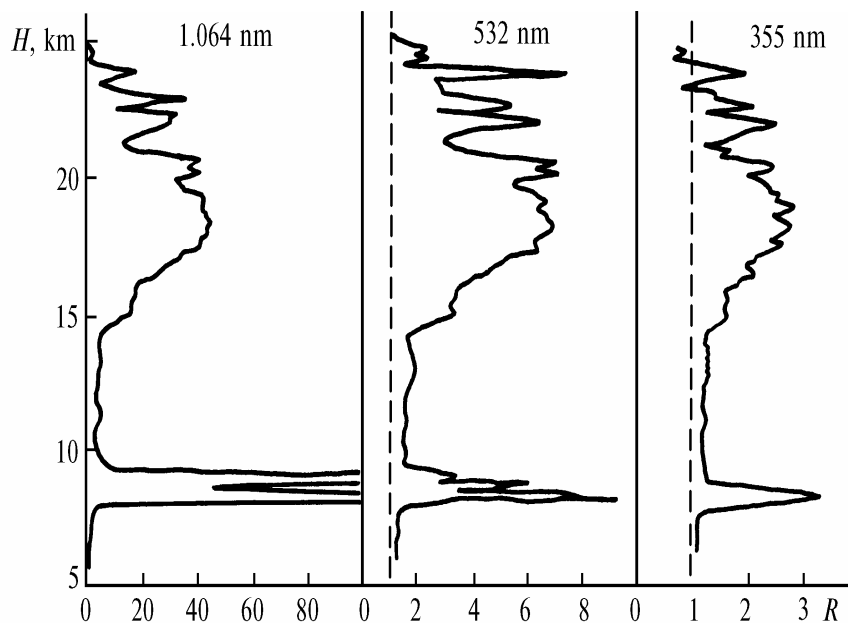


FIG. 10.

The measurements provide a distinct picture of a vertical aerosol structure and its variation from day to day. The maximum R values at 532 nm are close to those observed by Jäger at Garmisch-Partenkirchen in October 1991 and considerably smaller than those measured by Winker and Osborn at much lower latitudes. The three-wavelength measurements were used for determining the particle size distribution in order to improve the estimate of aerosol overburden in the stratosphere and the knowledge of microphysical and dynamic processes. The profiles of scattering ratio R were used to calculate the wavelength power spectral exponent α_{sp} in the aerosol backscatter spectral behavior. Comparison of the data at 1.064 and 0.355 μm yielded $\alpha_{sp} = 0.7-1.2$; and $\bar{\alpha}_{sp} = 1.0$. Insignificant variations in α_{sp} were observed in the altitude range 15–23 km. The values α_{sp} for the pair of wavelengths at 1.064 and 0.532 μm were found to be larger than those for the pair at 0.532 and 0.355 μm . These values are somewhat smaller than those measured by Post et al. in September 1991 (Ref. 8) who reported values of α about 1.5. A comparison of these values of α with those calculated for a sulphuric acid aerosol, using Mie theory, shows that a uniform size-distribution of aerosol up to radii at least a few tens of microns.

To provide for early detection of the effect of the Pinatubo eruption on the atmosphere, NASA arranged an airborne mission to survey the stratospheric plume soon after the eruption. An aircraft was equipped with depolarization lidar, all observations were made at the wavelength of 532 nm. Six flights were made during the period July 7–14 (21–28 days after the eruption). The measurement results were vertical profiles of R and depolarization δ reconstructed from the trajectories of flights accomplished to the southeast from Florida (0–35°N, 50–80°W). At early stages of the eruption the volcanic material was stratified and was horizontally inhomogeneous. Volcanic aerosol was observed at altitudes between 17 and 26 km, the vertical extent of the layer ranging from one to several kilometers. The aerosol was concentrated in two layers: at 22.5 km (0–5°S) and 25–26 km (from 2 to 13–14°N). The second layer was more dense with $R = 80$. The layering of the aerosol was associated with the wind shear (Fig. 11). Thus, the wind profile over Barbados, then

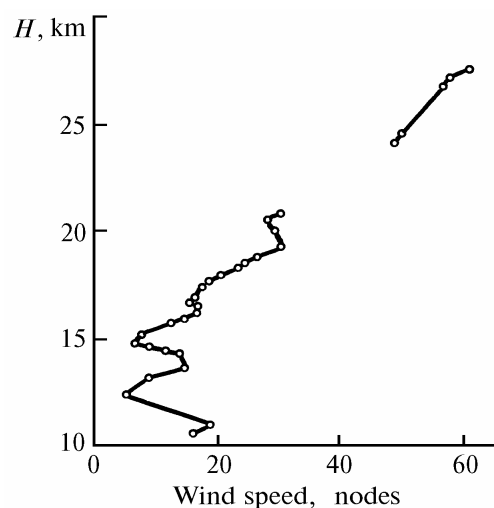


FIG. 11.

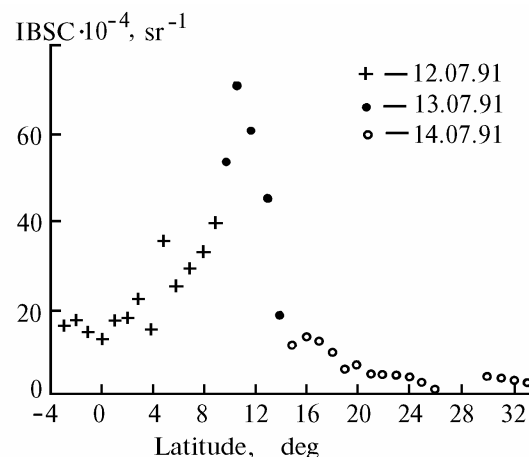


FIG. 12. Latitudinal variations of IBSC in the stratosphere (532 nm) observed during three successive days: July 12–13 (+), July 13 (●), and July 14 (○).

observed, indicated that aerosol in the layer at 25 km was transported more rapidly than in the lower layers. The data on wind speeds in the stratosphere and SAGE-II data confirmed that the layer at 25 km corresponded to the leading edge of the volcanic plume after 1.5 turn around the Earth since the eruption.

Figure 12 shows the IBSC values observed during the last three flights of the mission. The maximum aerosol content was observed on July 13, 1991 due to the dense layer at

25 km. Using a mass-to-backscatter conversion ratio of 17.3 g-sr/m, the stratospheric aerosol mass was estimated to be 8 megatonnes. The extension of the aerosol cloud was estimated using SAGE-II data. Since SO₂ injected into the stratosphere had only partially converted to aerosol, the eventual mass loading should be at least twice as large as the above estimate. The total stratospheric aerosol mass under background conditions was on the order of 0.1 megatonnes before eruption.

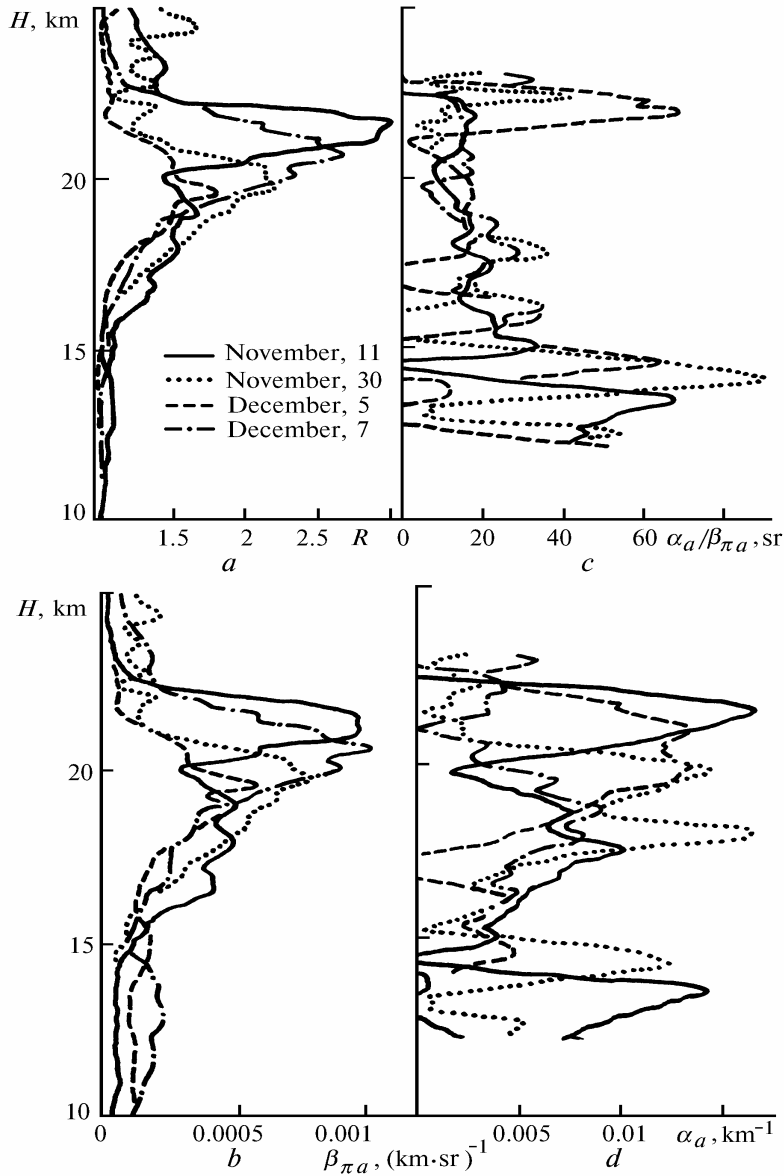


FIG. 13. Aerosol parameters derived from the lidar data at 351 nm. For (a) and (b) the vertical resolution is 300 m, for (c) and (d) it varies from 1.35 at 13 to 1.95 km at 23 km.

Multifrequency sensing of the Pinatubo stratospheric cloud was made at NASA/Goddard Space Flight Center. The measurements were carried out in November–December, 1991 using the Raman lidar with a XeF excimer laser. The

signals of elastic ($\lambda = 351$ nm) and Raman $\lambda = 3-72$ nm (O_2), $\lambda = 383$ nm (N_2), and $\lambda = 403$ nm (H_2O) backscatterers were detected.

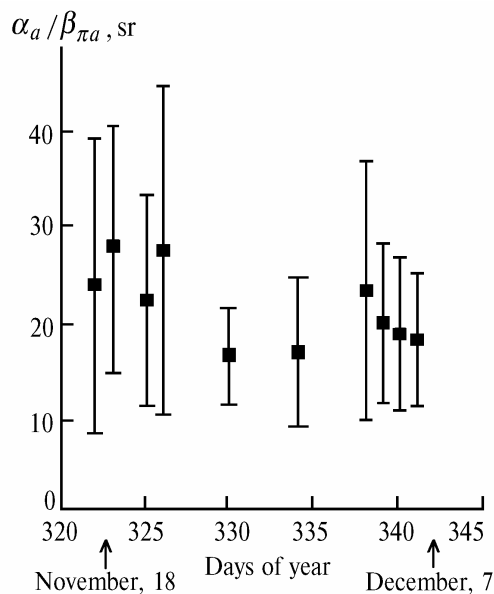


FIG. 14. The values $q = \alpha_a / \beta_{\pi a}$ obtained from lidar data at $\lambda = 351$ nm for the altitude range 15–25 km.

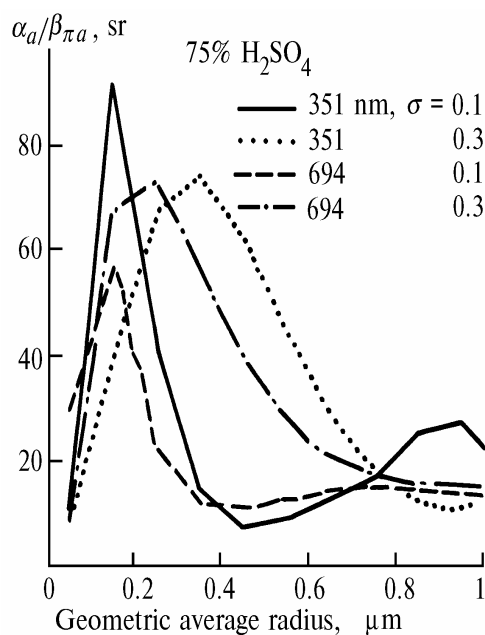


FIG. 15. The values $q = \alpha_a / \beta_{\pi a}$ calculated from Mie theory for spherical droplets consisting of 75% H_2SO_4 and 25% H_2O . The droplet size distribution is lognormal; standard deviations are $\sigma = 0.1$ and 0.3 .

The profiles of the aerosol scattering ratio R , coefficients of backward and total aerosol scattering ($\beta_{\pi a}$ and α_a), and lidar ratio $q = \alpha_a / \beta_{\pi a}$ at 10–25 km altitudes and 351 nm wavelength are presented in Fig. 13. According to the profiles of $\beta_{\pi a}$ and R , the maximum of aerosol concentration was between 19 and 22 km altitudes. The value q was calculated using Mie theory based on Raman signals and assuming the aerosols to be composed of

sulphuric acid droplets ($\text{H}_2\text{SO}_4 = 75\%$). These computations were made for 351 and 694 nm (Fig. 14). The value q ranges between 18–28 sr for altitudes between 15 and 25 km. Estimates of the modal radii of El Chichon and Pinatubo aerosols indicate that they generally range between 0.2 and 0.5 μm (Fig. 15). These values correspond to the lidar ratio $q = 10$ –30 sr. The wavelength dependences of the backscattering and extinction coefficients for such a size–distribution are $\alpha \sim \lambda^{-0.6}$, $\beta_{\pi} \sim \lambda^{-1.7}$, in the spectral regions near 351 and 694 nm.

Vertical distribution of q depicted in Fig. 13 can be explained by variations in particle size. Thus, following Fig. 15, q increases with particle size decreasing to 0.2 μm . The decrease of β_{π} at altitudes below 20 km (Fig. 13) indicates that the mean particle radius decreases to a typical size of 0.1 μm what corresponds to their background size–distribution. Then the lidar ratio should increase to $q = 50$ –60 sr as shown in Figs. 13 and 15.

The main bulk of aerosol was in the layer between 15 and 25 km with its maximum somewhere between 21 and 23 km. The aerosol optical thickness varied between 0.04 to 0.06.

THE VOLCANIC STRATOSPHERIC LAYER OVER ASIA

The volcanic stratospheric layer was observed at lidar stations of Japan (Hachioji, Tsukuba, Fukuoka), China (Hefei, Reking), Russia (Tomsk), and Belorussia (Minsk).

The measurements in Fukuoka (33.5°N, 130.4°E) made with the lidar at 532 nm wavelength in July 1991 detected strong scattering layers appeared in the stratosphere due to the Mt Pinatubo eruption.¹¹ These layers, by their aerosol loading, are comparable to aerosol layers from the El Chichon volcano. Similar to the El Chichon event two layers were observed: the lower layer about 17 km at the initial stage from July to August and the upper layer at heights between 20 and 35 km. The heights of the peaks of layers coincided with the heights of three temperature intervals. In some cases the temperature inversion occurred at the same altitude as a strong scattering layer.

The parallel sensing of the stratospheric aerosol cloud from the Pinatubo eruption was made at lidar stations of Tsukuba (36.05°N, 140.13°E) and Naha (26.20°N, 127.68°E). The observation at Tsukuba has been carried out continuously during a long time prior to the eruption and that at Naha started on September 19, 1991. The volcanic cloud had reached to Tsukuba about two weeks after the eruption in the form of an aerosol layer over the tropopause (Fig. 16a). Then in July and early August a dense and thin layer could be seen at the altitude of about 21 km which was then observed at about 21–27 km altitude. The layer grew day by day. The layer between 30 and 33 km appeared over Naha in the middle of November and similar kind of layer was also seen at Tsukuba a few days later.

The integrated backscattering coefficient (Fig. 17a) in the stratosphere over Tsukuba was gradually increasing since the end of September till the end of February 1992. The same coefficient over Naha (Fig. 17b) also increased by the middle of November coinciding by time with the first observation of the upper layer above 30 km. In December the IBSC decreased to the value of the beginning of observations in Naha while strong fluctuations of the IBSC observed in Tsukuba in December and January. These phenomena may reflect the variations in the wind field in the stratosphere and in the processes of aerosols transportation from lower to higher latitudes.

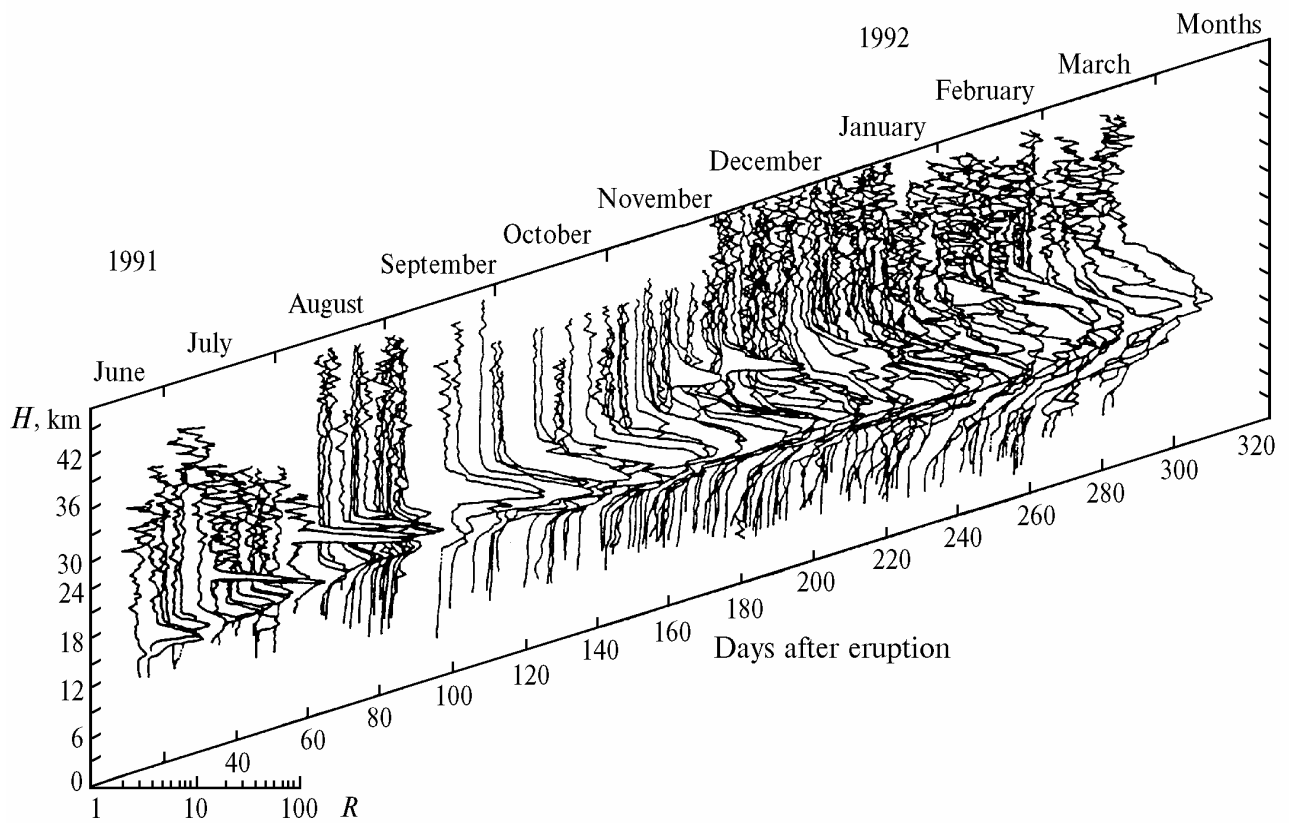


FIG. 16 a. Profiles of R observed at Tsukuba late in June 1991 to mid of March 1992.

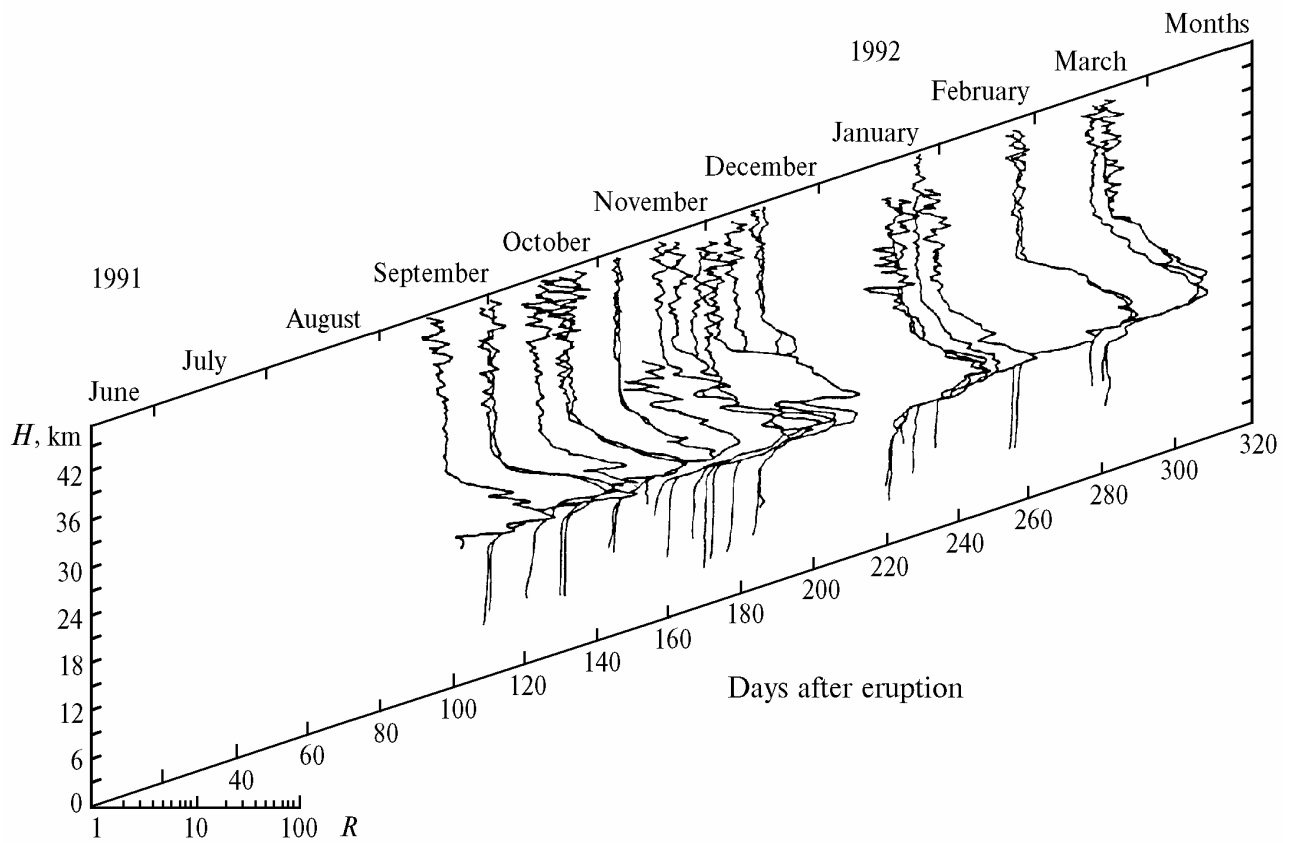


FIG. 16 b. The same as Fig. 16 a but at Naha in the mid of September 1991 till the mid of March 1992.

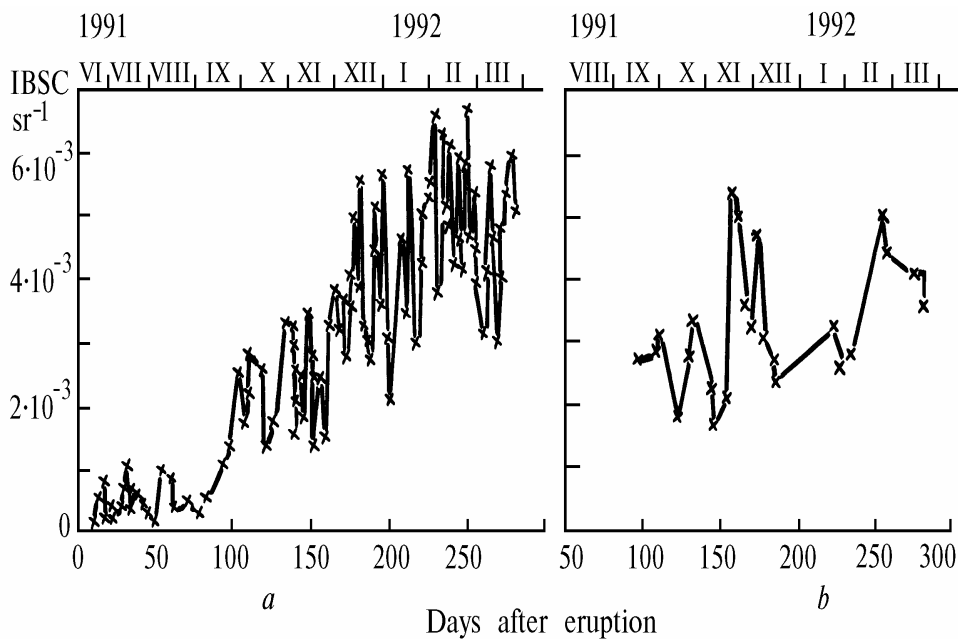


FIG. 17. Time variation of IBSC at Tsukuba (a) and at Naha (b).

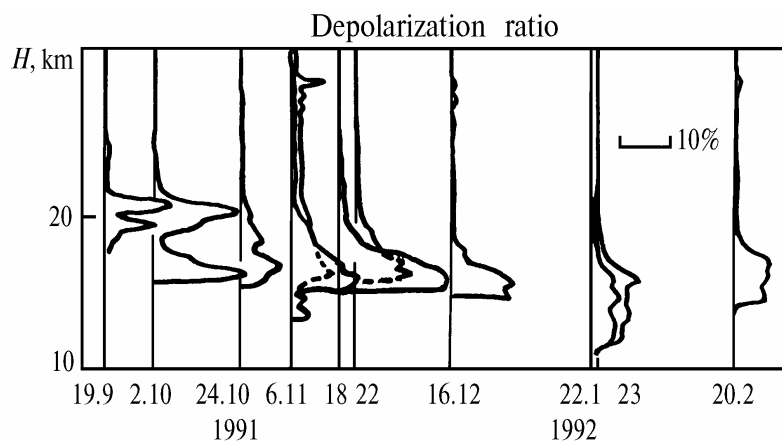


FIG. 18 a. Profiles of δ of the stratospheric aerosol at Naha.

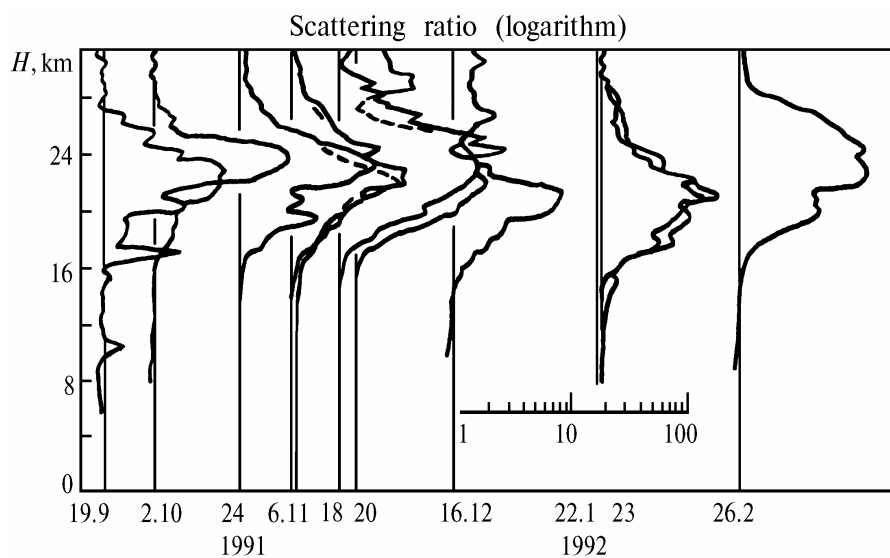


FIG. 18 b. Profiles of R used to calculate actual values of δ for aerosol by separating out the depolarized backscatter of the atmospheric molecules from the total backscatter depolarization.

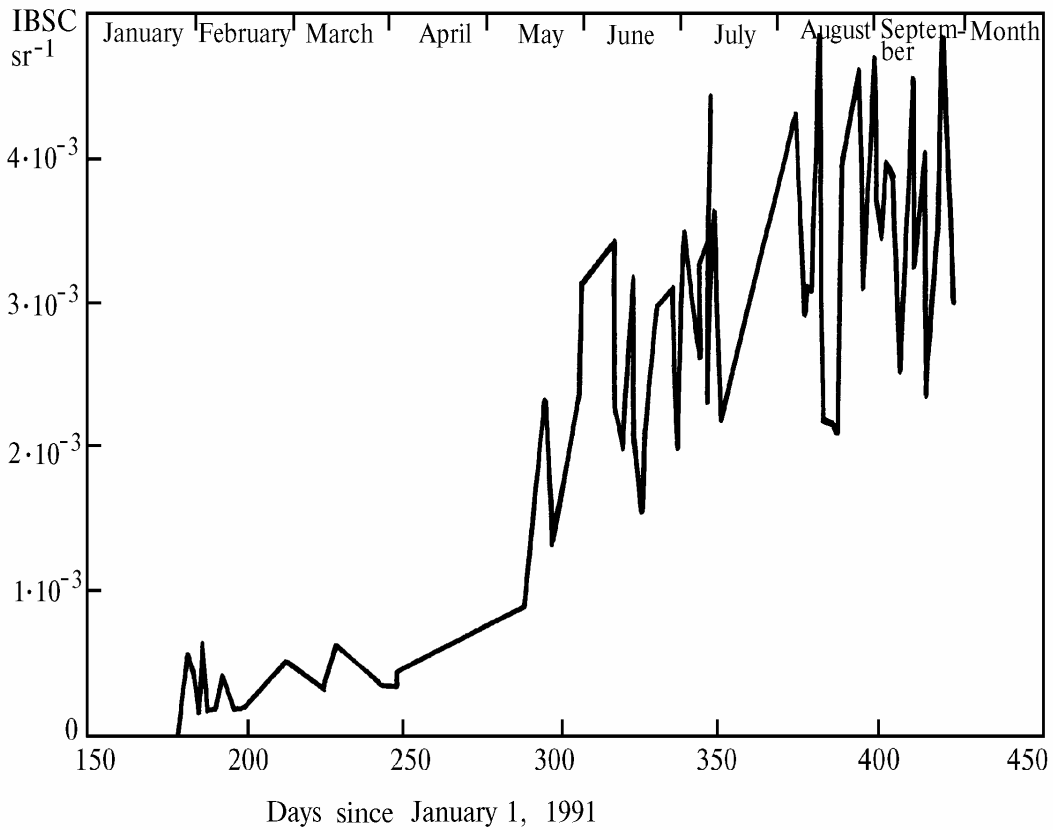


FIG. 19. Temporal behavior of IBSC at $\lambda = 532$ nm within the altitude range 15–30 km.

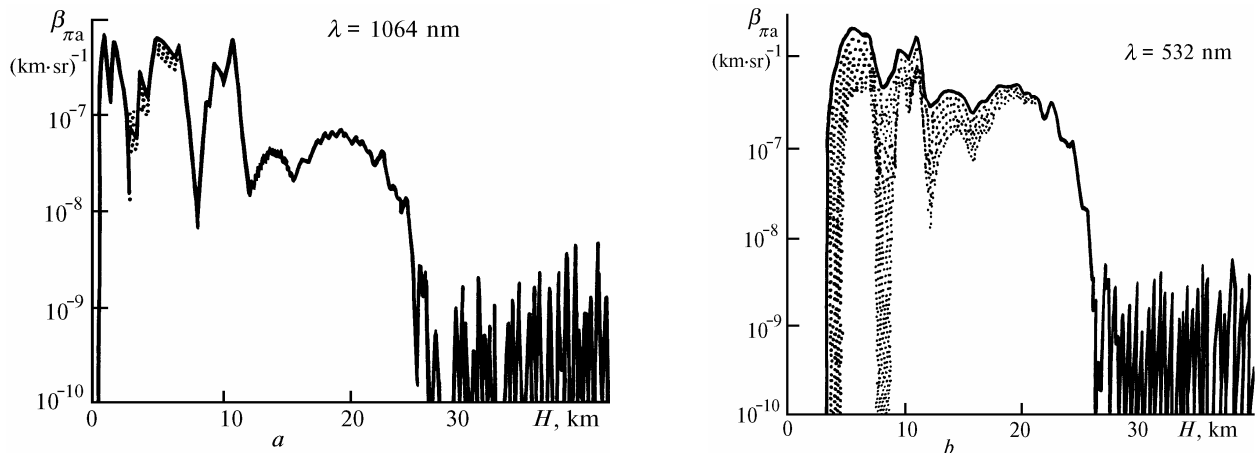


FIG. 20. Profiles $\beta_{\pi a}$ corrected for attenuation due to extinction by aerosols using the Fernald equation: 1064 (a) and 532 nm (b). The corrected profiles with $q = 10$ (top) to $q = 90$ (bottom) are shown by dots. The solid curve is for the case of no correction used for extinction ($q = 0$).

The data of polarization observations are depicted in Fig. 18. Presented here are the profiles of depolarization ratio and corresponding profiles of scattering ratio. The largest depolarization ratios are observed at the bottom of the aerosol cloud with the depolarization peak descending gradually. Thus it can be stated that nonspherical particles causing the radiation depolarization were in the lower part of the aerosol cloud while the spherical ones being in its upper part. The nonspherical particles could be considered to be the volcanic ash and the spherical ones to be the product of chemical reactions of SO_2 .

Multifrequency lidar measurements of the aerosol layer from Mt. Pinatubo eruption have also been carried out at NIES, Tsukuba. Two lidar systems were used: the big NIES lidar (532 nm) and three-wavelength lidar (1064, 532, and 535 nm) operating since June, 1991. Temporal variations of IBSC obtained with the NIES lidar are shown in Fig. 19. It is seen from the figure that the main body of aerosol clouds first came over Japan at the end of 1991 although some aerosol formations sporadically appeared since a half month after the eruption. Analysis of optical properties of the atmosphere was made using the lidar data

obtained since December, 1991 when the main body of the aerosol cloud started to appear over Japan. The following aerosol parameters were determined: extinction-to-backscatter ratios, spectral dependence of these coefficients, and optical thickness.

The backscattering coefficients were calculated using preset values of the lidar ratio $q = \alpha/\beta_{\pi a}$. Figure 20 depicts the $\beta_{\pi a}$ profiles at 1064 and 532 nm obtained for different values of q .

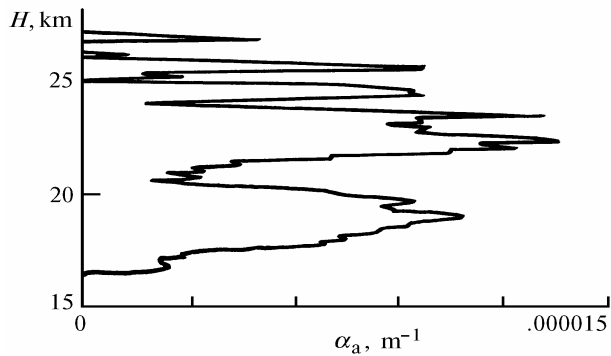


FIG. 21.

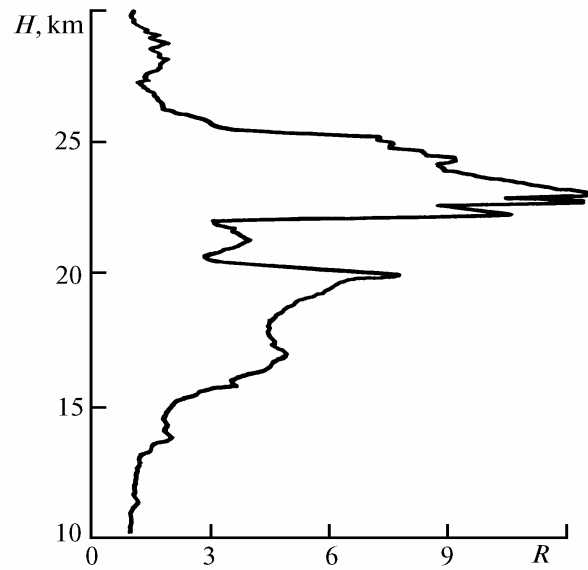


FIG. 22.

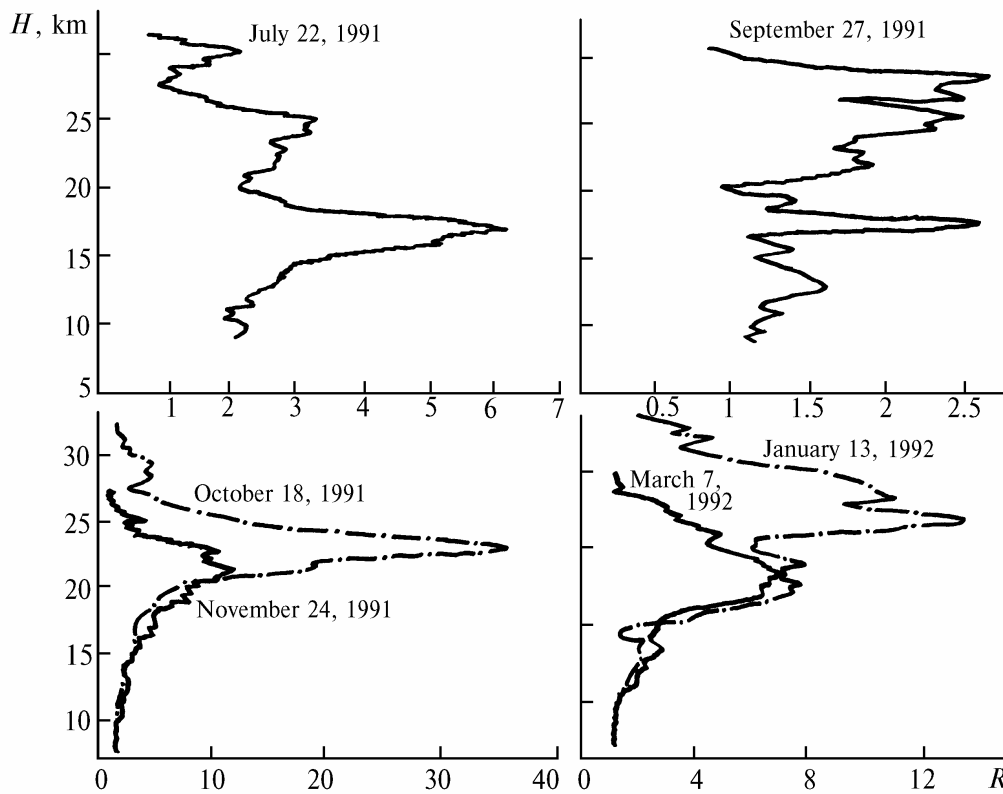


FIG. 23.

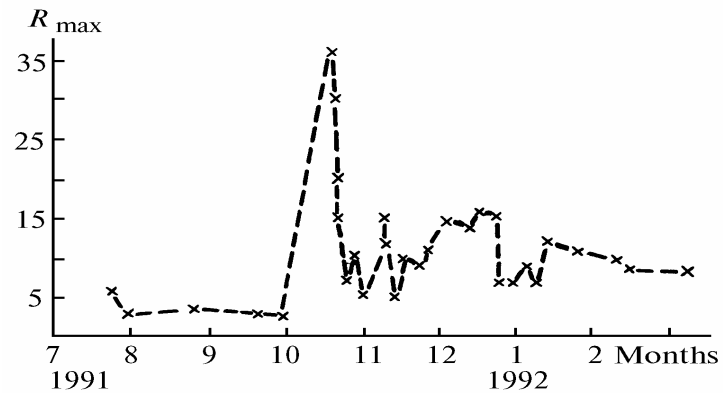


FIG. 24.

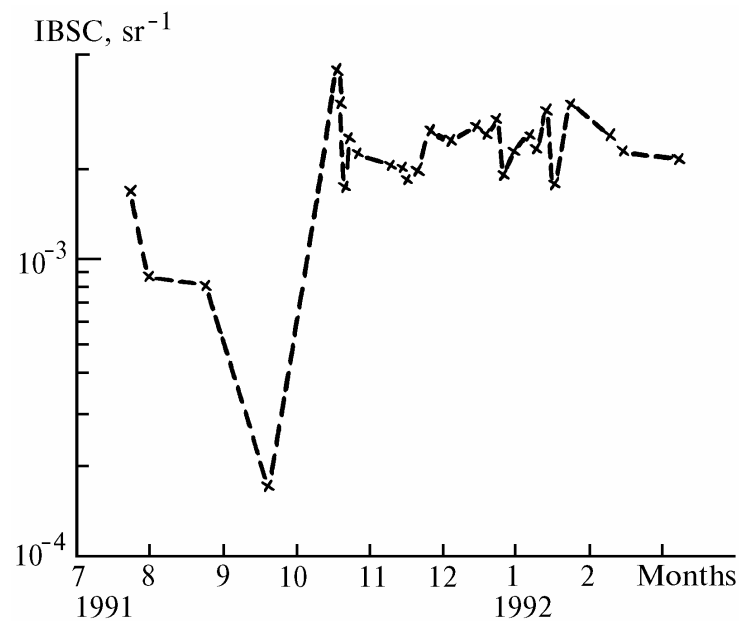


FIG. 25.

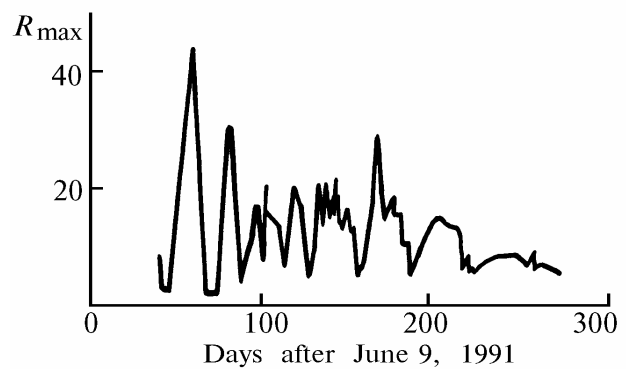


FIG. 26.

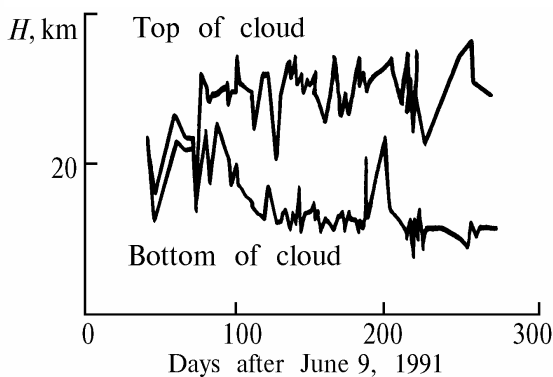


FIG. 27.

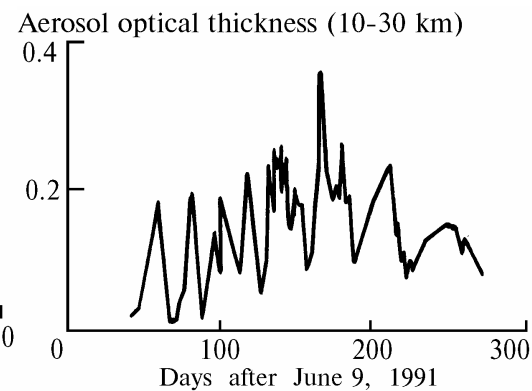


FIG. 28.

Based on the measurement data obtained during the period from December 1991 till March 1992 the powers of the spectral dependencies were determined for the coefficients of backscattering $\delta(\beta_{\pi_1} = \beta_{\pi_2} (\lambda_1/\lambda_2)^{-\delta})$ and total scattering $\gamma(\alpha_1 = \alpha_2 (\lambda_1/\lambda_2)^{-\gamma})$. The values of δ and γ for 355 and 532 nm were 1.4 and 1.6, respectively. The optical thickness τ at $\lambda = 532$ nm at altitudes between 15 to 30 km was 0.104.

The two-wavelength measurements of the extinction coefficient profiles of stratospheric aerosol from the Pinatubo volcano were made using a Raman lidar at Tokyo University in Hachioji. The two-wavelength measurement technique¹⁴ used elastic ($\lambda_L = 532$ nm) and Raman ($\lambda_R = 607$ nm – vibrational Q-branch of nitrogen) scattering what made it possible to reconstruct the extinction coefficient profiles $\alpha(532$ nm). Assuming the wavelength dependence of the aerosol extinction coefficient in the form

$$\alpha_a(\lambda_L = 532)/\alpha_a(\lambda_R = 607) = \lambda_R/\lambda_L$$

we obtain that the profile of the aerosol extinction coefficient is

$$\alpha_a(\lambda_L, H) = \frac{1}{1 + \lambda_L/\lambda_R} \left\{ \frac{d}{dH} \ln \frac{N(H)}{H^2 P(H)} - \alpha_{Lm} - \alpha_{Rm} \right\}$$

where $N(H)$ is the molecular density at an altitude H ; α_{Lm} and α_{Rm} are the molecular scattering coefficients. The profiles of extinction coefficient and scattering ratio obtained on February 23, 1992 are shown in Figs. 21 and 22. The sounding data reveal a pronounced structure of the volcanic aerosol with two layers at altitudes between 15 to 20 and 22 to 25 km, respectively.

In China the observations of stratospheric clouds after the Pinatubo eruption were made over Peking (39.54°N, 116.27°E) and Hefei (31.32°N, 117.17°E). The measurements over Peking were conducted using a ruby laser ($\lambda = 694$ nm) which delivered 0.5–1.0 J/pulse and a 40 cm – diameter Cassegrainian telescope. Spatial resolution¹⁵ was 0.3 km. During the period from July 22, 1991 till March 7, 1992 the value of R at $H = 15$ to 20 km increased to 2.5–6 by September, 1991 (Fig. 23). A double-layer structure having maxima at altitudes between 25 to 27 and 16 to 17 km was observed since September. On October 16, 1991 a sudden increase of R to 37 was detected in the upper layer at the altitude range 20–25 km. Temporal behavior of the maximum scattering ratio R_{\max} and the integrated backscattering coefficient (15–30 km) for nine months is depicted in Figs. 24 and 25.

In Hefei the observations were carried out using a lidar with a Nd:YAG laser ($\lambda = 532$ nm) delivering 120 mJ per pulse, a receiving telescope of 625 mm diameter, and a photon counting recording system.¹⁶ Eighty four scattering

ratio profiles in the volcanic cloud have been obtained at altitudes between 6 and 35 km with the spatial resolution 600 m during the period between July 19, 1991 and March 8, 1992.

Figure 26 shows variations in R_{\max} during 300 days after the Pinatubo eruption. The values of R varied in a wide range from 2.0 to 44.1 (August 8) in the period from July 19 till September 5. The volcanic cloud was first observed in Hefei 40 days after the Pinatubo eruption and was extremely inhomogeneous in the beginning. The cloud top expanded slightly from 21 to 25 km during the first 33 days (Fig. 27), and then kept nearly the same level at 25 km. But the cloud bottom descended slowly and steady from about 20 km to 15 km.

On the 80th day after the eruption the optical depth was almost one order of magnitude larger than that before the eruption (Fig. 28). There is close correlation between optical depth and the maximum of scattering ratio. The optical depth was mainly determined by a dense part of the cloud.

The observations of stratospheric volcanic clouds were made in Russia at the Institute of Atmospheric Optics, Russian Academy of Sciences (Tomsk, 56.4°N, 89°E) and in Belorussia at the Institute of Physics, Belorussian Academy of Sciences (Minsk, 54°N, 27°E). The results of lidar sensing of stratospheric aerosol over Tomsk and Minsk before and after the Pinatubo eruption are described at length in some papers of this special issue of the journal.

REFERENCES

1. J.S. Bluth Gregg, D. Doiron Scott, Ch.C. Schnetzler, A.J. Krueger, and L.S. Walter, *Geophys. Res. Lett.* **19**, 151–154 (1992).
2. A. Ansmann, Ch. Schulze, et al., in: *Abstracts of Papers at 16th ILRC*, MIT, July 20–24 (1992), pp. 7–10.
3. H. Jäger and D. Hofmann, *Appl. Opt.* **30**, 127–138 (1991).
4. F. Congeduti, A. Adriani, et al., in: *Abstracts of Papers at 16th ILRC*, MIT, July 20–24, (1992), pp. 79–81.
5. W. Steinbrecht, D. Donovan, and A.I. Carswell, *ibid.*, pp. 87–90.
6. M.T. Osborn, D.M. Winker, et al., *ibid.*, pp. 91–94.
7. G.S. Kent, G.M. Hansen, K.M. Skeens, *ibid.*, pp. 71–74.
8. M.J. Post, C.J. Grund, A.O. Langford, M.H. Proffit, *Geophys. Res. Lett.* **19**, 195–198 (1992).
9. D.M. Winker, M.T. Osborn, et al., in: *Abstracts of Papers at 16th ILRC*, MIT, July 20–24 (1992), pp. 67–70.
10. R.A. Ferrare, S.H. Melfi, et al., *ibid.*, pp. 13–16.
11. T. Nagai, O. Uchino, and T. Fujimoto, *ibid.*, pp. 17–20.
12. Y. Sasano, I. Matsui, and S. Hayashida, *ibid.*, pp. 75–78.
13. M. Abo and Ch. Nagasawa, *ibid.*, pp. 11–12.
14. A. Ansmann, M. Ribesell, and C. Weitkamp, *Optics Lett.* **15**, No. 13, 746–748 (1990).
15. S. Jinhui, Q. Jinhuan, et al., in: *Abstracts of Papers at 16th ILRC*, MIT, July 20–24 (1992), pp. 243–245.
16. Hu. Huanling and Jun Zhou, *ibid.*, pp. 83–86.